The Review Of
DIABETIC
STUDIES OPEN ACCESS

Enhanced Anticancer Activity Of Taxifolin Via Niosomal Encapsulation In MCF-7 Breast Cancer Cells

Nourah Abdullah Al-Aifan[1], Fayez Mohmmed Alyahya[2], Saleh Suleiman Al-Abdulatif[3], Nasser Abdulla Alarifi[4], Alanoud Mubarak Abdullah Alruways[5], Abdullah Saad Alomeery[6], Saad Abdulaziz Alnasser[7], Rasha Mohammed Faisal Alhamyani[8]

[1]Medical Laboratories, Dawadmi General Hospital, Riyadh Third Health Cluster, Riyadh, Saudi Arabia
[2,3,3]Laboratory Technician, Dawadmi General Hospital, Riyadh Third Health Cluster, Riyadh, Saudi Arabia
[5]Pharmacist, Dawadmi General Hospital, Riyadh Third Health Cluster, Riyadh, Saudi Arabia
[6]Dawadmi General Hospital, Riyadh Third Health Cluster, Riyadh, Saudi Arabia
[7]Dawadmi General Hospital, Health Information Technician Cluster, Saudi Arabia
[8]Psychologist, Children Hospital in Taif, Taif Health Cluster, and Specialist-Laboratory, Saudi Arabia

Abstract

Background: Though taxifolin is a naturally occurring flavonoid with autoantioxidant capabilities and some reported anticancer effects, its real-world applications are still limited due to its instability and poor bioavailability. Niosomes, as a nanodelivery system, are expected to enhance delivery effectiveness. This investigation aimed to evaluate the potential chemoprotective and pro-apoptotic effects of taxifolin-loaded niosomes (Tax-NIO) in MCF-7 breast cancer cells.
Methods: The thin-film method was used to prepare the niosomes, which were characterized for morphology, size, and polydispersity index (PDI). The drugs loaded niosomes were subjected to entrapment efficiency (EE) and stability, and drug release studies. We further evaluated the impact of Taxifolin on the viability of breast cancer cells, RT-qPCR assays, malondialdehyde (MDA) activity, and cell cycle progression.
Results: Tax-NIO has a small size of approximately 51 ± 0.40 nm, a low PDI of 0.132 ± 0.14, and a zeta potential of -21 ± 0.23 mV, indicating stability. There was a continuous release of drugs in comparison to unencapsulated taxifolin. In a dose-dependent manner, Tax-NIO caused a drop in MCF-7 cell viability, and its IC_{50} was 48.9 µM, which was higher than the 23.4 µM IC_{50} for olaparib. Upregulation of pro-apoptotic genes such as p53, Bax, Caspase-9, and Caspase-3 was observed, whereas anti-apoptotic genes Bcl-2 and PARP-1 were downregulated. Tax-NIO resulted in a significantly lower level of lipid peroxidation. Cell cycle analysis also showed there was significant G2/M phase arrest in the Tax-NIO-treated cells.
Conclusions: Incorporation of taxifolin into niosomes exhibits even greater anticancer effects against MCF-7 breast cancer cells, including increased apoptosis, greater inhibition of oxidative stress, and greater disruption of cell-cycle progression. Thus, these findings indicate that Tax-NIO could serve as an effective nanotherapeutic strategy for breast cancer and warrant further preclinical and translational studies.

Keywords: Taxifolin, Niosome, Breast cancer cells, Cell cycle analysis, apoptosis

1 Introduction

Antioxidants, whether natural or synthetic, are utilized in food to mitigate the initial stages of oxidation-induced deterioration. Currently, consumers prefer natural products to avoid artificial additives. Taxifolin (3,3′,4′,5,7-pentahydroxiflavanon, or dihydroquercetin) is a bioactive compound classified under the flavanone subgroup; it is present in citrus fruits, red onions, milk thistle, seeds of the species Silybum, and pine wood, among other sources. Taxifolin exhibits structural and functional similarities to quercetin and rutin (1,2).

It contains a hydroxyl group at the C-3 position of the C ring. The structural distinction between quercetin and taxifolin lies in the presence of a 2,3 double bond in quercetin, which is associated with its potent antioxidant activity. In contrast to other antioxidant compounds commonly used in the food industry, such as ascorbic acid, taxifolin exhibits robust antioxidant activity. It applies to edible oils, beef, lard, poultry fats, dry milk powder, and chilled salmon. The pharmacological actions reported include radioprotective, anti-inflammatory, antiviral, and antitumor properties. It has been demonstrated to exhibit anticancer, antibacterial, and antitumor effects, enhance immunological functions, and protect against cardiovascular disorders. Owing to the aforementioned qualities, taxifolin can be used in a diverse array of applications, including food additives, health foods, pharmaceuticals, and other related goods. Despite its extensive biological activities, the use of taxifolin in food formulations is limited primarily by its low water solubility (0.87–1.00 mg mL−1 at 25 °C) (3,4).

The hydrophobic nature of taxifolin and its reduced solubility rate in watery gastrointestinal fluids frequently lead to insufficient bioavailability. Other researchers enhanced taxifolin bioavailability by reducing particle size with Liquid Antisolvent Precipitation (LAP) technology. Micronized taxifolin was synthesized using supercritical antisolvent (SAS) technology in previous investigations. The granule shape was predominantly needle-like, with a particle size ranging from 2 to 11 μm (5).

It may be inferred that nanocarriers enhance bioavailability, phenolic functionality, and the bioactive properties of other compounds due to their significantly larger surface area. Nanoparticles can readily traverse cell membranes. Nanoparticles enter target cells, thereby releasing their cargo. Various preparation methods have been employed to manufacture nanocapsules with distinct characteristics in terms of size, polydispersity index (PDI), and encapsulation efficiency (EE) (6).

Niosomes are generated through the self-assembly of non-ionic surfactants in aqueous conditions, leading to the organization of surfactant macromolecules into bilayers. Niosomes and their manufacturing process, like liposomes, are formed by the adverse interactions between surfactants and water molecules. Furthermore, they can capture hydrophilic and amphiphilic molecules. Various surfactants have been employed in the formulation of nonionic vesicles for the potential delivery of bioactive nanovesicles (7).

The most critical tumor suppressor gene is p53. p53 is a key biomarker in cancer, and elevated p53 expression may improve patient prognosis (8). Bcl-2-Associated X Protein (Bax) is a member of the B-cell lymphoma 2 (Bcl-2) protein family and is essential for regulating cellular apoptosis and survival. Overexpression of Bax induces apoptosis, underscoring the necessity of stringent regulation of Bax from transcription through post-translational modification for cellular survival. Bcl2 is a crucial protein that regulates apoptosis. The highly varied expression in many hematological malignancies offers protection against cell death induced by oncogenic and environmental stresses. The initiation and conclusion of apoptosis are significantly aided by members of the caspase family (9,10).

Various cancer therapies promote apoptosis by indirectly activating these caspases, resulting in the demise of cancer cells. Poly(ADP-ribose) polymerase-1 (PARP-1) is involved in several critical biological processes, including apoptosis, regulation of cell proliferation, replication, and DNA damage repair (11). Various cancer cell types exhibit elevated PARP-1 levels, and this overexpression has been associated with tumor growth (10).

Olaparib is a small molecule PARP inhibitor that mitigates the effects of ionizing radiation and alkylating agents on DNA when administered orally. The FDA has sanctioned the PARP inhibitor olaparib (Lynparza) for the treatment of adult patients with deleterious or presumed detrimental gBRCAm, HER2-negative metastatic breast cancer who have undergone chemotherapy in the neoadjuvant, adjuvant, or metastatic contexts (12).

This work sought to elucidate the chemoprotective effects of Tax-NIO in in vitro cancer models by evaluating its capacity to induce apoptosis in MCF-7 breast cancer cells and by examining the mechanisms underlying this effect.

2. Materials and Methods

Chemicals

Taxifolin was purchased from Sigma Aldrich (St. Louis, MO, USA). Preparation of Tax NIO took place at the Nanomaterials Research and Synthesis Unit, Animal Health Research Institute (ARC, Giza, Egypt). From LKT Laboratories (St. Paul, MN, USA), Olaparib was purchased. Cell lines were obtained

from the National Research Centre, Giza, Egypt. All remaining chemicals used in the experiment were obtained from Sigma-Aldrich (St. Louis, MO, USA).

Preparation of Tax-NIO

In the thin-film approach (13) to produce niosomes, 20 mg of cholesterol and 100 mg of Span 60 in 10 mL of chloroform were mixed, and the resulting solution was dried using a rotary evaporator (Buchi R-3, Switzerland). Niosomes containing Tax were made by adding the film to the Tax Solution. To obtain a concentration of 50 mg/ml, Tax was added to 10 mL of Phosphate-Buffered Saline (PBS; pH 7.4) at 60°C. Sonication of the aqueous solution and dispersion of the lipid layer was performed in an ultrasonic bath (Sonics & Materials Inc., USA) at 60 Hz and room temperature for 15 min.

Characterization of Tax-NIO

Zeta potential, Polydispersity Index, and Morphology

For the purpose of measuring the niosomes' size, polydispersity index, and zeta potential values, the DLS, Malvern Zetasizer, Nano ZS model, Malvern Instruments LTD, U.K., was used, and it was the DLS that provided the results. Each sample underwent triplicate analysis. The Tex-NIO templates analysis was complemented by digital micrograph and SoftImageViewer, which were used to analyze the sample using the transmission electron microscope (JEOL JEM-2100; JEOL LTD, Tokyo, Japan). One drop from the niosomal dispersion was diluted with deionized water in a 1:10 ratio and left on a carbon-coated copper grid for a minute, where it was meant to help the niosomes adhere. They were unembedded and unstained for TEM examination, though they were first dried to room temperature (14).

Entrapment Efficiency (EE)

Using the direct method, the ability of Tax-NIO formulations to retain was determined. By suspending the lyophilized Tax-NIO in ethanol, then vortexing and centrifuging, the Tax-NIO encapsulation efficiency (EE%) was assessed. A 205 nm UV spectrophotometer was used to determine the drug concentration, and the drug's EE was calculated from the standard curve (15). The methodology requires that the EE of a substance be expressed as a percentage to meet the standard (% EE drug).

$$\text{Drug EE (\%)} = \frac{\text{Wi} - \text{Wf}}{\text{Wi}} \text{x} 100$$

Wi is the concentration of the drug initially in the niosome preparations, and Wf is the concentration of the drug present in the weighted amount of the loaded niosome at the end.

Drug Release Study

A dialysis bag (MWCO = 12 kDa) containing 2 milliliters of the free drugs Tax-NIO for drug release (in vitro) was used. The dialysis bag was inserted into 50 milliliters of phosphate-buffered saline (PBS) (1X, pH = 5.4, pH = 7.4) and centrifuged at 37 degrees Celsius. Supernatant samples were collected at predetermined time points and replaced with fresh PBS.

Stability Studies

To study Tax-NIO's stability, we placed them in two different settings simultaneously. They were maintained at 25 ± 1 °C and 4 ± 1 °C for 3 months. The average physical parameters (mean particle size (nm), PDI, EE) were measured at the end of the study period and at 0, 1, 2, and 3 months.

Cell Culture

At the standard conditions of 37°C, 5% CO2, and sub-confluence, MCF-7 cells were cultured in complete Roswell Park Memorial Institute-1640 medium fortified with 10% FBS, penicillin/streptomycin, and L-glutamine (Sigma-Aldrich, St. Louis, MO, USA).

In vitro cytotoxicity

The MTT assay (3-(4,5-dimethylthiazol-2-yl)-2,5-diphenyl-2H-tetrazolium bromide) is a colorimetric assay where yellow MTT is converted to purple formazan. The following steps were done in a clean environment in a Laminar flow cabinet complying with biosafety level II (Baker, SG403INT, Sanford,

ME, USA), where l04 cells/well were exposed to different concentrations of Tax-NIO (5, 10, 25, 50, and 100 µM) and olaparib (5, 10, 25, 50, and 100 µM) (16). After 2 days, 2.5 µg/ml MTT was added to each well, and the plates were incubated for an additional 4 hours at 37°C. After the formazan crystals were formed, the crystals were dissolved by adding 200 µl/well of 10% sodium dodecyl sulfate, and the absorbance was measured at 595 nm using a positive control, which is known to cause 100% mortality under the same experimental conditions. The following equation was used to calculate the percentage change in viability.

Cytotoxicity %= (Extract reading/Negative control reading) x 100,

Viability %= 100- Cytotoxicity%,

The impact of each treatment is measured by its IC50 (the concentration that reduces cell viability by 50%).

Quantitative RT-PCR analysis

Using an Ambion RNA Mini Kit (Life Technologies; catalog number 12183018A), RNA from the cells was extracted. To assess sample quality, we used a NanoDrop® ND-1000 Spectrophotometer (Wilmington, Delaware, USA). To prepare the cDNA, a High-Capacity cDNA Reverse Transcription Kit (4374966) from Thermo Scientific was used. For the real-time PCR assay (17), the Maxima SYBR Green qPCR Master Mix (2×) from Thermo Scientific (catalog #K0251) was used. For the controls, housekeeping gene GADPH was selected. To calculate target gene expression levels, the 2^-ΔΔCt method was used (18). The primer pairs for the target genes are listed in Table 1.

Table 1. Primers sequences

Gene	Primers	Accession number
P_{53}	F 5′- CCTCAGCATCTTATCCGAGTGG-3′ R 5'-TGGATGGTGGTACAGTCAGAGC-3′	NM_000546
Bax	F 5′- TCAGGATGCGTCCACCAAGAAG -3′ R 5'- TGTGTCCACGGCGGCAATCATC -3′	NM_001291428
Bcl2	F 5′- ATCGCCCTGTGGATGACTGAGT-3′ R 5'- GCCAGGAGAAATCAAACAGAGGC-3′	NM_000633
Caspase-9	F 5′-GTTTGAGGACCTTCGACCAGCT-3′ R 5'-CAACGTACCAGGAGCCACTCTT-3′	NM_001229
Caspase-3	F 5′- GGAAGCGAATCAATGGACTCTGG-3′ R 5'-GCATCGACATCTGTACCAGACC-3′	NM_004346
PARP 1	F 5′- CCAAGCCAGTTCAGGACCTCAT-3′ R 5'- GGATCTGCCTTTTGCTCAGCTTC-3′	NM_001618
GAPDH	F 5′- GTCTCCTCTGACTTCAACAGCG -3′ R 5'- ACCACCCTGTTGCTGTAGCCAA -3′	NM_001256799

Detection of lipid peroxidation

To establish baseline levels of lipid peroxidation, we seeded 2 × 10 cells/ml into 96-well culture plates. After 48 hours of exposure to Tax-NIO (48.9 µM) and olaparib (23.4 µM), the cells were harvested and washed twice with PBS. We harvested the cells using an ice sonic probe (VCX-130 W, Newtown, USA). We disrupted the cells by ultrasonication for 5 seconds. In accordance with the manufacturer's protocol, we measured malondialdehyde (MDA) in the cell extract using the MDA test kit. We assessed MDA content using a microplate reader set to 532 nm (Tecan, Männedorf, Switzerland) (19).

Cell cycle stage detection

Cells were seeded at 2 × 10 cells/ml per well in 100-mm plates overnight in fresh culture medium. The following day, Tax-NIO and olaparib treatment started for 48 hours. After cell harvest, cells were fixed

by incubation in 70% ethanol at 20°C for 12 hours. Later, the cells were treated with RNase (10 mg/mL) and propidium iodide (50 μg/mL) for 30 min. The data were analyzed using FlowJo software (TreeStar, Ashland, OR, USA) to evaluate cell-cycle distribution (20).

Statistical analysis

GraphPad Prism 5 (GraphPad Software, La Jolla, CA, USA) was used for all statistical analyses. For comparisons of more than two groups, one-way analysis of variance (ANOVA) was used, followed by Tukey's test for statistically significant differences. All graphs show the mean value +/- the standard error (SE) of three or more independent observations. The statistical significance threshold was set at $p < 0.05$.

3. Results

Tax-NIO characterization

Morphological characterization

The average particle size, PDI, and zeta potential were measured by dynamic scattering light analysis using the Malvern Zetasizer. In Tax-NIO, the average size was 51 ± 0.40 nm. The PDI value was 0.1321±0.14, which is considered in the acceptable range. The ZP value of Tax-NIO was -21±0.23 mV (Figure 1).

Figure 1. Characterization of Tax-NIO TEM image.

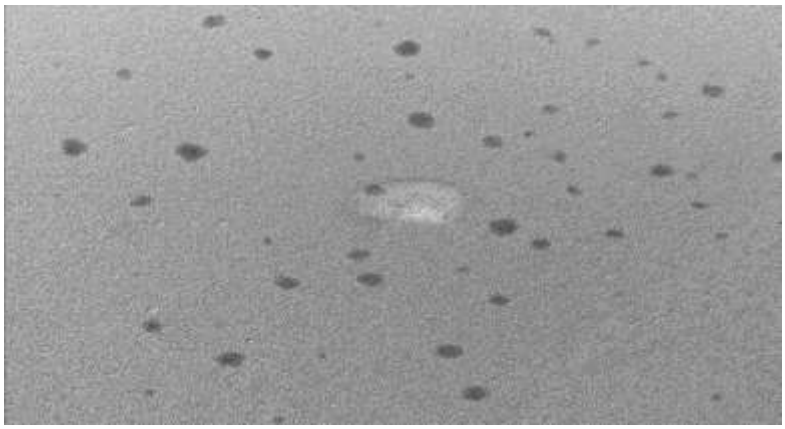

Drug release studies of Taxifolin from niosomes

Taxifolin formulation's drug release profile was studied for 48 hours at pH 5.4 and pH 7.4 at 37°C to learn more about in vitro drug release. As can be observed in the "Release" plot (Figure 2), at pH 5.4 and pH 7.4, the Taxifolin free medications saw a rapid increase in release (42%, 50.31% over the first six h); after 12 h, the rate of release was (66%, 81.3%). After 24 h, the rate of release was increased to (82.3%, 93%). According to monitoring of the Tax-NIO release profile at pH 5.4 and 7.4, 20.6% and 24.3% of the drug were released, respectively, after 6 hours.

Figure 2. In vitro drug release profile of Tax and Tax-NIO from the dialysis bag in pH 5.4 and pH 7.4 at 37 °C. The mean and SD of 3 samples are displayed.

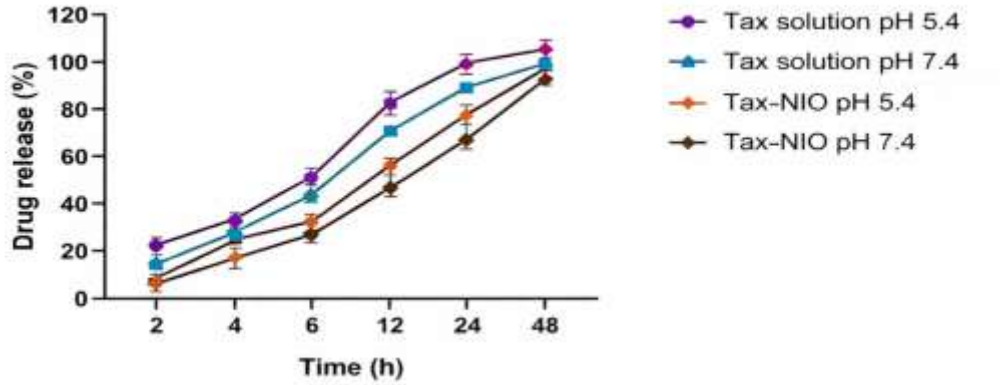

Physical stability study of Tax-NIO

Weights, sizes, PDIs, and EEs of Tax-NIO bilosomes were measured at both frozen and room temperatures at baseline and at 1, 2, and 3 months to evaluate their stability and effectiveness. Notably, there was no discernible effect of temperature on Tax-NIO size, PDI, or EE; however, at baseline, the Tax-NIO size was the smallest (59 nm), with a PDI of 0.174 and an EE of 87.1%. According to the stability graph (Figure 3), temperature was a contributing factor in months 1-3. There was an increase in size and PDI, and a decrease in EE. 25 °C was the cause of the increase in size and PDI and the reduction in EE. The EE was inversely proportional to the amount of drug released. Stiffness, elasticity, and temperature can affect the decrease in PDI and the increase in EE of niosome pores. The 3-month sample at 4 °C had the smallest particle size, and the lowest EE was 71.6%. At 25 °C, the developed pores increased in size, PDI, and, by the third month, reduced EE (61.67%), indicating that the niosomes are stiffer and more elastic at lower temperatures.

Figure 3. Tax-NIO alone at 4 °C and 25 °C was compared for mean annealing temperature stability. Stability parameters being mean particle size (A), PDI (B), and % EE (C). Data are reported as mean ± SD (n =3). *P<0.05.

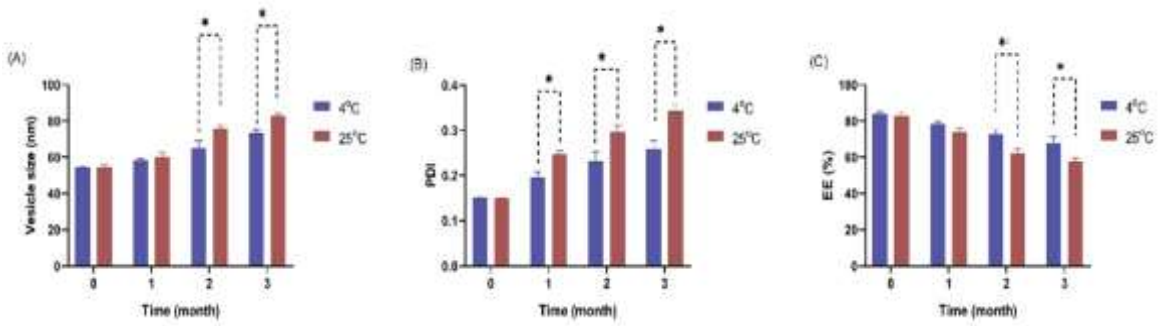

Cytotoxic impact on MCF-7 cells

In Figure 4, the viability% of MCF-7 cells was significantly reduced after 48 hours of incubation with Tax-NIO and olaparib at different concentrations. Moreover, Tax-NIO exhibited cytotoxic activity against both cell types, with IC50 values of 48.9 µM and 23.4 µM for olaparib, respectively (Figure 4).

Figure 4. The impact of varying concentrations of Tax-NIO, Tax, and olaparib on MCF-7 cells' viability using the MTT assay following 48 hours of incubation. Results displayed are mean±SEM, p < 0.05.

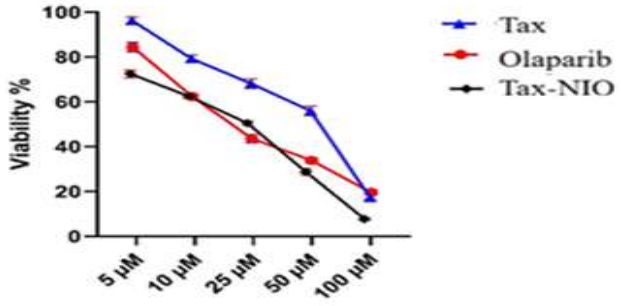

Evaluation of the mRNA expression levels of marker genes in MCF-7 cells

The expression of p53, Bax, caspase-9, and caspase-3 in Tax-NIO-, Tax-, and olaparib-treated MCF-7 cells was compared with that in untreated cancer cells. There was a marked upregulation in expression of the listed mRNAs, and it was found that Tax-NIO-treated MCF-7 cells and olaparib-treated MCF-7 cells showed mRNA expression levels of caspase-9 and caspase-3 that were statistically similar. There were also comparable levels of caspase-3 expression between untreated and Tax-treated cancer cells (Figure 5).

Figure 5. The MCF-7 cell lines most affected by Tax-NIO, Tax, and olaparib were those with altered expression levels of the genes P53 (A), Bax (B), caspase-9 (C), and caspase-3 (D) (mRNA expression normalized to GADPH). * Indicates statistical significance when compared to the untreated group ($p < 0.05$).

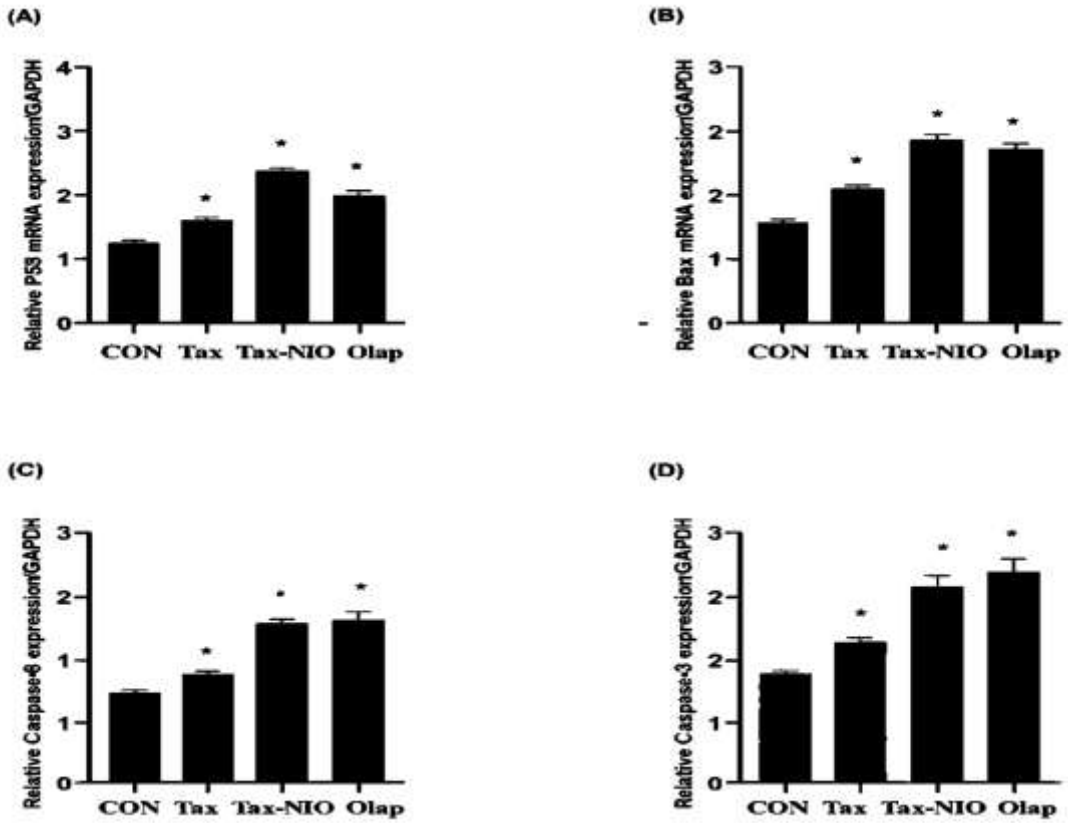

In contrast to our previous results, the expression levels of anti-apoptotic Bcl2, PARP 1, were significantly the highest transcriptional level in untreated cancer cells, while the cells treated with Tax-NIO, Tax, and olaparib revealed significant downregulation in Bcl2, PARP 1 in MCF-7 cells in comparison with the untreated cancer cells (Figure 6).

Figure 6. The effects of Tax-NIO, Tax, and olaparib on the gene expression levels of Bcl2 (A), PARP 1 (B), (Relative gene mRNA expressions/GADPH) in the MCF-7 cell lines. * Statistically significant difference between control and treated group ($p < 0.05$)

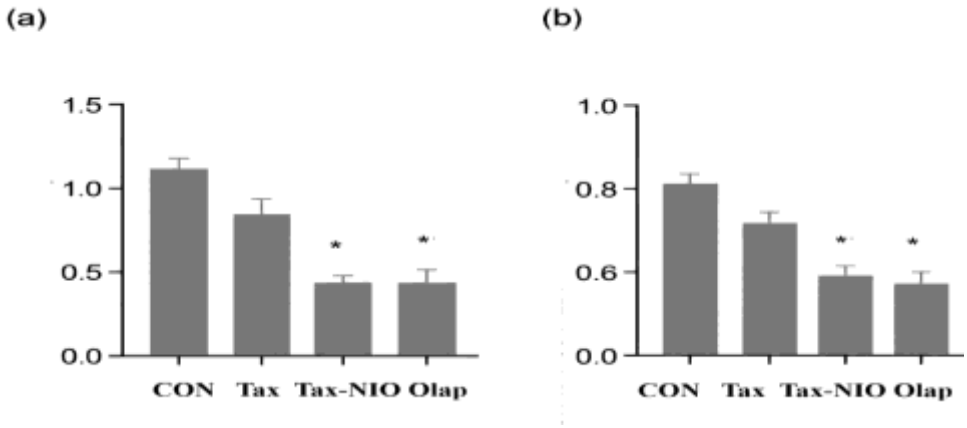

Evaluation of lipid peroxidation marker (MDA)

In contrast, untreated cancer cells have much higher MDA than MCF-7 cells treated with olaparib, Tax-NIO, or MCF-7 (Figure 7).

Figure 7. The influence that Tax-NIO, Tax, and olaparib conversely have on the amount of MDA (nmol/mg) within the MCF-7 cell lines. * There is a statistically significant difference between the control and the treated group ($p < 0.05$)

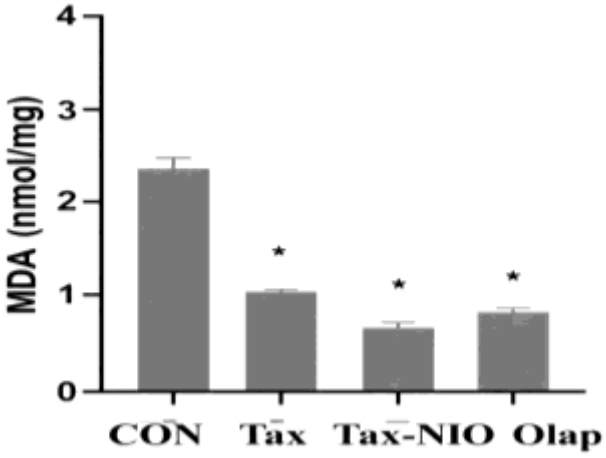

Analysis of the cell cycle

We hypothesized that Tax-NIO- and Tax-induced apoptosis involved cell-cycle interruption and thus evaluated the cell-cycle distribution following Tax-NIO and Tax treatment. Breast cancer MCF-7 cells treated with Tax-NIO for 48 h revealed a significant ($p < 0.05$) increase in the number of cells arrested at the G2/M (15.3%) phase, and the proportion of cells in the G0/1 phase (47.0%) was decreased in comparison with untreated cancer cells as well as cells treated with Tax showed a significant increase in the number of cells arrested at the G0/1 (67.5%) phase. The proportion of cells in S phase (1.0%) was lower than in untreated cancer cells. In cells treated with olaparib, our data showed a significant increase in the number of cells arrested at G0/1 (63.2%). In contrast, the proportion of cells in S phase (8.6%) was lower than in untreated cancer cells (Figure 8).

Figure 8. Effect of Tax-NIO, Tax, and olaparib on the cell cycle progression of breast cancer MCF-7 (A). * Significance of differences between control and treated group ($p < 0.05$),

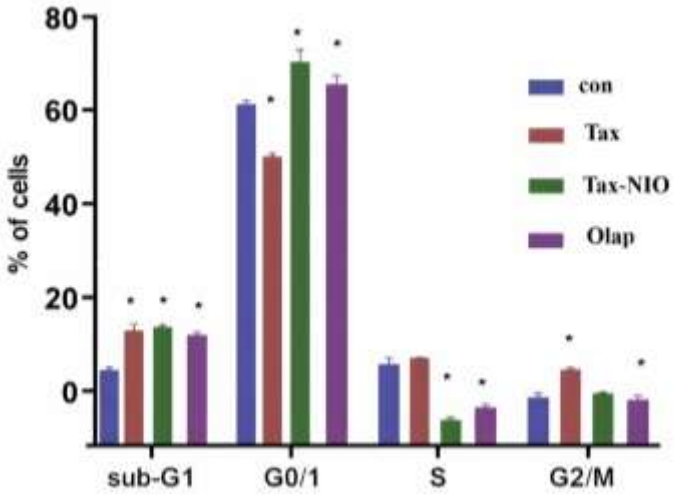

4. Discussion

One of the main contributors to worldwide illness and death is cancer, which involves the proliferation of cells, the inhibition of apoptosis, genetic instability, and changes to the body's oxidation and reduction reactions. There have certainly been remarkable improvements in breast cancer treatment. There is also the development of targeted therapies. Yet, off-target effects, treatment resistance, and systemic toxicity still restrict therapeutic success. These obstacles have led to investigations into adjunct strategies to improve the efficacy of therapeutic interventions while avoiding serious side effects. This is especially the case when one considers the use of adjunct therapies that target one or more oncogenic pathways (21).

Because of their safety, human use history, and mechanisms of action, the anticancer properties of sweet cherry flavonoids, natural products derived from plants, make them promising. Unfortunately, the clinical use of flavonoids has not been realized. This is due to their poor aqueous solubility, low bioavailability, rapid metabolism, and low cellular uptake. Anticancer effects of flavonoids also arise from their ability to stimulate apoptosis and reduce inflammation and metastasis. To reduce these obstacles, plant compounds in medicine can have their therapeutic effects amplified by employing niosomes. These drug delivery systems improve drug stability, enhance release, and improve delivery and targeting to tumors (compared to standard approaches) (5-7).

Taxifolin (dihydroquercetin) is an anticancer agent, according to recent results, against multiple cancer types. Taxifolin has been shown to modulate apoptosis, cell proliferation, and cell migration. Changes in oxidative stress and blockade of central cell signaling pathways, such as PI3K/Akt, Wnt/β-catenin, NF-κB, and mTOR, also suppress tumor growth. Furthermore, taxifolin can alter multidrug resistance in cancer cells, making it a potential candidate as a chemosensitizer (23).

The goal of this study was to evaluate the anticancer potential of taxifolin encapsulated in niosomes (Tax-NIO) against the highly proliferative MCF-7 breast cancer cells. We proceeded to study and analyze the specific physicochemical properties of Tax-NIO, such as controlled release behavior, cytotoxic activity, and the subsequent release of downstream apoptosis-related genes and alterations in oxidative stress, regarding the progression of the cell cycle in comparison to the free taxifolin drug versus the standard of care (SOC) drug, olaparib.

The tax-NIO formulation exhibited nanoscale dimensions, low polydispersity, a weakly negative zeta potential, and good stability. The formulation exhibited sustained-release, release-dependent release, and acceptable stability, making it likely to serve as a nanocarrier system for intracellular delivery of taxifolin.

Taxifolin was reported by Chen et al. to cause uncompetitive inhibition of P-glycoprotein, thereby resensitizing multidrug-resistant cells to gain intracellular drug retention and chemosensitivity (21). Consistent with these findings, our results showed that Tax-NIO, rather than free taxifolin, induced MCF-7 cell death in a dose-dependent manner. This increased cytotoxicity in MCF-7 cells was greater

than that of free taxifolin (owing to the niosomal system's enhanced sustained cell uptake and release), supporting the aforementioned idea of sustained cell uptake and release.

In the same way, taxifolin was shown to inhibit the tumor-promoting mechanisms leading to the proliferation, migration, and invasion of osteosarcoma cells (22). Our findings that Tax-NIO induced cell cycle arrest, indicating decreased cancer cell proliferation, and that Tax-NIO, compared with free taxifolin, showed enhanced anti-cancer activity than expected for nanotechnology, indicate that the anti-cancer activity of flavonoids was enhanced by nanotechnology. This observation supports the notion that greater efficacy of Tax-NIO in free taxifolin indicates the role.

Das and others compiled evidence demonstrating taxifolin's ability to modulate multiple pathways implicated in apoptosis, oxidative stress, and cancer-promoting mechanisms (23). Our results confirm this, as Tax-NIO induced upregulation of pro-apoptotic genes (p53, Bax, caspase-9, and caspase-3) while simultaneously repressing anti-apoptotic genes (Bcl-2 and PARP-1), indicating activation of the intrinsic mitochondrial apoptotic pathway. Most importantly, the apoptotic response induced by Tax-NIO was comparable to that caused by olaparib, further underscoring the potential of Tax-NIO in cancer treatment.

Haque and others (24) showed the pathway in which taxifolin inflicts an anti-mammary carcinogenic effect, and this is via the deregulation of the LXR/mTOR/PTEN pathway (24). Following these mechanistic pathways, we observed significant progress in apoptosis and in the suppression of survival pathways in Tax-NIO-treated MCF-7 cells. This suggests that the taxifolin nanoformulation can target dysregulated signaling pathways in breast cancer.

Carcinogenesis is associated with oxidative stress, and one of the most dangerous forms of oxidative stress is Reactive Oxygen Species (ROS). ROS are involved in DNA damage, the regulation of cell survival and death, and other aspects of cellular regulation. MDA is a potent and dangerous carcinogen and is a marker for the type of lipid peroxidation caused by ROS, and is used in the assessment of severe illnesses, namely cancer, to evaluate oxidative stress. In several types of cancer, MDA levels and, consequently, lipid peroxidation in cancer cells are elevated. MDA is a major contributor to cellular aging and is implicated in cell death. The MDA is a functional intermediate that promotes cell growth during periods of oxidative stress. When MDA is formed during metabolism, it reacts with amino groups, which supports the hypothesis that these changes are responsible for cell growth. In the production of excess ROS, mechanisms for the type of DNA damage, inherited mutations, and loss of cell function are destroyed. Furthermore, redox control in tumor and normal cells under stress differs. This is one of the reasons for the high sensitivity of tumor cells to oxidative stress. One of the suggested treatments focuses on oxidative stress, which is used to explain the high sensitivity of tumor cells. This treatment of cancer cells focuses on redox control, as these cells are susceptible to stress and fragile. The combination of heightened metabolic stress and rapid cellular division causes the stress-regulating capacity of these cells to stagnate at inefficient levels. Consequently, increased production of highly reactive oxygen species leads to further DNA damage and reduced cell viability (25, 26).

Hossain and Ray characterized the mechanisms by which taxifolin triggered epigenetic regulation of p53 and apoptotic genes in Ewing's sarcoma (27). Likewise, the current study demonstrated pronounced upregulation of p53 and other mediators of apoptosis after tumors received Tax-NIO, indicating that cells would produce or accumulate higher intracellular concentrations of taxifolin and possibly rekindle or restore previously silenced p53 pathways.

Li et al. established the fact that taxifolin was able to decrease the migration and invasion of breast cancer cells through β-catenin signaling and was able to induce the mesenchymal to epithelium transition (28). Although migration was not assessed in the study, Tax-NIO induced G2/M cell cycle arrest and triggered apoptosis, consistent with a less aggressive tumor phenotype and reduced tumor growth and activity.

Lin et al. claimed that taxifolin was responsible for breast cancer reduction by amplifying the cancer-targeting $CD8^+$ T cells and regulating the tumor suppressor genes (29). While immune modulation was out of the scope of the in vitro, the strongly pronounced anti-proliferative and pro-apoptotic effects of taxifolin demonstrated with Tax-NIO suggest that the nano-delivery of taxifolin in more elaborate tumor microenvironments would increase taxifolin’s anti-cancer potential.

Manigandan et al. established that taxifolin prevented colon carcinogenesis by inhibiting the NF-κB-mediated Wnt/β-catenin signaling pathway and activating Nrf2 (30). The decreased oxidative stress and

increased apoptosis observed in the aforementioned findings reflect taxifolin's dual action as a redox-modulating anticancer agent, consistent with the dual anti-proliferative and antioxidant mechanisms.
Oi et al. illustrated that taxifolin inhibited skin carcinogenesis induced by UV radiation through modulating the signaling of EGFR and PI3K (31). Our study built on and confirmed prior findings by demonstrating that Tax-NIO disrupts critical survival pathways in breast cancer cells, leading to apoptosis and cell cycle arrest. Overall, these findings substantiate the considerable improvement in taxifolin's anticancer activities through niosomal encapsulation and bring taxifolin to the forefront of innovative therapeutic interventions in breast cancer (32,33).
Insights from Haque and Pattanayak's studies also indicated that taxifolin impairs the development of breast cancer from the exposure of DMBA through modulation of the AhR/CYP1A1 pathways (25,26). Our research corroborates these results by showing that Tax-NIO significantly attenuated oxidative stress, as evidenced by a reduction in MDA levels in treated cells. The balance of oxidative stress is consistent with the protective effect of taxifolin, which has been documented to alleviate oxidative damage induced by carcinogens and to strengthen its protective role against lipid peroxidation in breast cancer cells.
The oral PARP inhibitor olaparib is therapeutically impactful in patients with recurrent ovarian cancer and a breast cancer gene (BRCA) mutation. People who have human epidermal growth factor receptor 2-negative, metastatic breast cancer and a hereditary BRCA mutation benefited greatly from switching to olaparib monotherapy rather than the standard treatment, with olaparib monotherapy extending median progression-free survival by 2.8 months and reducing the risk of death (34).

5. Conclusions

Overall, taxifolin-loaded niosomes (Tax-NIO) displayed promising anticancer activity against MCF-7 breast cancer cells, thanks to their nanoscale features (tiny particle size, acceptable PDIs, negative zeta potentials) alongside a sustained release profile, acceptable short-term (especially at refrigeration) stability, dose-dependent cytotoxicity, and noticeable pro-apoptotic activity (increased P53/Bax/caspases and reduced Bcl-2 and PARP-1/Bcl-2), lower levels of the peroxidation marker MDA, and cell cycle arrest (most noticeably G2/M), similar to or better than performance of olaparib with respect to some apoptotic activity. Tax-NIO has to undergo wider angiogenesis, arising from (1) establishing clinical activity and selectivity in other subtypes of breast cancer and in its regular cell counterparts, (2) enhancement of formulation consistency, stability, and preservation (especially at 4°C), and reduction of batch-to-batch variability, (3) and comprehensive pharmacological testing in animals and tissue to assess toxicity and clinical activity, before it can be considered as a condensed nanocarrier in a novel anticancer technique.

Funding: This research received no external funding.

Data Availability Statement: The data supporting the findings of this study are available within the article.

Conflicts of Interest: The authors declare no conflict of interest.

Reference

1. Lobo, V., Patil, A., Phatak, A., & Chandra, N. (2010). Free radicals, antioxidants, and functional foods: Impact on human health. Pharmacognosy reviews, 4(8), 118.
2. Khlupova, M., Vasil'eva, I., Shumakovich, G., Morozova, O., Chertkov, V., Shestakova, A., ... & Yaropolov, A. (2016). Laccase-mediated biotransformation of dihydroquercetin (taxifolin). Journal of Molecular Catalysis B: Enzymatic, 123, 62-66.
3. Osorio, E., Pérez, E. G., Areche, C., Ruiz, L. M., Cassels, B. K., Flórez, E., & Tiznado, W. (2013). Why is quercetin a better antioxidant than taxifolin? Theoretical study of mechanisms involving activated forms. Journal of Molecular Modeling, 19(5), 2165-2172.
4. Topal, F., Nar, M., Gocer, H., Kalin, P., Kocyigit, U. M., Gülçin, İ., & Alwasel, S. H. (2016). Antioxidant activity of taxifolin: an activity–structure relationship. Journal of enzyme inhibition and medicinal chemistry, 31(4), 674-683.

5. Sun, X., Chen, R. C., Yang, Z. H., Sun, G. B., Wang, M., Ma, X. J., ... & Sun, X. B. (2014). Taxifolin prevents diabetic cardiomyopathy in vivo and in vitro by inhibition of oxidative stress and cell apoptosis. Food and Chemical Toxicology, 63, 221-232.
6. Haleem, A., Javaid, M., Singh, R. P., Rab, S., & Suman, R. (2023). Applications of nanotechnology in the medical field: a brief review. Global Health Journal, 7(2), 70-77.
7. Bhardwaj, P., Tripathi, P., Gupta, R., & Pandey, S. (2020). Niosomes: A review on niosomal research in the last decade. Journal of Drug Delivery Science and Technology, 56, 101581.
8. Kaloni, D., Diepstraten, S. T., Strasser, A., & Kelly, G. L. (2022). BCL-2 protein family: Attractive targets for cancer therapy. Apoptosis.
9. Wolf, P., Schoeniger, A., & Edlich, F. (2022). Pro-apoptotic complexes of BAX and BAK on the outer mitochondrial membrane. Biochimica et Biophysica Acta (BBA) – Molecular Cell Research, 119317.
10. Boice, A., & Bouchier-Hayes, L. (2020). Targeting apoptotic caspases in cancer. Biochimica et Biophysica Acta (BBA) – Molecular Cell Research, 1867, 118688.
11. Kumar, M., Jaiswal, R. K., Yadava, P. K., & Singh, R. P. (2020). An assessment of poly(ADP-ribose) polymerase-1 role in normal and cancer cells. BioFactors, 46, 894–905.
12. Andreidesz, K., Koszegi, B., Kovacs, D., Bagone Vantus, V., Gallyas, F., & Kovacs, K. (2021). Effect of oxaliplatin, olaparib and LY294002 in combination on triple-negative breast cancer cells. International Journal of Molecular Sciences, 22, 2056.
13. Moghaddam, Z. S. (2024). A novel drug delivery system incorporates a functional composite scaffold derived from taxifolin with potential cytotoxic and anticancer effects on triple-negative breast cancer.
14. Darwesh, A. Y., El-Dahhan, M. S., & Meshali, M. M. (2021). A new dual function orodissolvable/dispersible meclizine HCL tablet to challenge patient inconvenience: In vitro evaluation and in vivo assessment in human volunteers. Drug Delivery and Translational Research.
15. Bae, Y. H., & Park, K. (2021). Advanced drug delivery 2020 and beyond: Perspectives on the future. Advanced Drug Delivery Reviews, 158, 4–16.
16. Ashmawy, A. M., Sheta, M. A., Zahran, F., & Abdel Wahab, A. H. (2017). MiRNAs-181a/b as predictive biomarkers for olaparib sensitivity in triple-negative breast cancer cells. BLJ, 13, 221–229.
17. Livak, K. J., & Schmittgen, T. D. (2001). Analysis of relative gene expression data using real-time quantitative PCR and the 2−ΔΔCT method. Methods, 25, 402–408.
18. Livak, K. J., & Schmittgen, T. D. (2001). Analysis of relative gene expression data using real-time quantitative PCR and the 2−ΔΔCT method. Methods, 25, 402–408.
19. Gérard-Monnier, D., Erdelmeier, I., Régnard, K., Moze-Henry, N., Yadan, J. C., & Chaudiere, J. (1998). Reactions of 1-methyl-2-phenylindole with malondialdehyde and 4-hydroxyalkenals: Analytical applications to a colorimetric assay of lipid peroxidation. Chemical Research in Toxicology, 11, 1176–1183.
20. Mei, L., Sang, W., Cui, K., Zhang, Y., Chen, F., & Li, X. (2019). Norcantharidin inhibits proliferation and promotes apoptosis via c-Met/Akt/mTOR pathway in human osteosarcoma cells. Cancer Science, 110, 582–595.
21. Sarg, N. H., Hersi, F. H., Zaher, D. M., Hamouda, A. O., Ibrahim, S. I., El-Seedi, H. R., & Omar, H. A. (2024). Unveiling the therapeutic potential of Taxifolin in Cancer: From molecular mechanisms to immune modulation and synergistic combinations. Phytomedicine, 133, 155934.
22. Newman, D. J., & Cragg, G. M. (2020). Natural products as sources of new drugs over the nearly four decades from 01/1981 to 09/2019. Journal of Natural Products, 83(3), 770–803.
23. Peer, D., Karp, J. M., Hong, S., Farokhzad, O. C., Margalit, R., & Langer, R. (2007). Nanocarriers as an emerging platform for cancer therapy. Nature Nanotechnology, 2(12), 751–760.
24. Das, A., Baidya, R., Chakraborty, T., Samanta, A. K., & Roy, S. (2021). Pharmacological basis and new insights of taxifolin: A comprehensive review. Biomedicine & Pharmacotherapy, 142, 112004.
25. Chen, H.-J., Chung, Y.-L., Li, C.-Y., Chang, Y.-T., Wang, C. C. N., Lee, H.-Y., Lin, H.-Y., & Hung, C.-C. (2018). Taxifolin resensitizes multidrug resistance cancer cells via uncompetitive inhibition of P-glycoprotein function. Molecules, 23(12), 3055.

26. Chen, X., Gu, N., Xue, C., & Li, B.-R. (2018). Plant flavonoid taxifolin inhibits the growth, migration and invasion of human osteosarcoma cells. Molecular Medicine Reports, 17(2), 3239–3245.
27. Hossain, M. M., & Ray, S. K. (2014). EWS knockdown and taxifolin treatment induced differentiation and removed DNA methylation from p53 promoter to promote expression of Puma and Noxa for apoptosis in Ewing's sarcoma. Journal of Cancer Therapy, 5(12), 1092–1113.
28. Li, J., Hu, L., Zhou, T., Gong, X., Jiang, R., Li, H., Kuang, G., Wan, J., & Li, H. (2019). Taxifolin inhibits breast cancer cells proliferation, migration and invasion by promoting mesenchymal to epithelial transition via β-catenin signaling. Life Sciences, 232, 116617.
29. Lin, X., Dong, Y., Gu, Y., Kapoor, A., Peng, J., Su, Y., Wei, F., Wang, Y., Yang, C., Gill, A., Neira, S. V., & Tang, D. (2023). Taxifolin inhibits breast cancer growth by facilitating CD8+ T cell infiltration and inducing a novel set of genes including potential tumor suppressor genes in 1q21.3. Cancers, 15(12), 3203.
30. Manigandan, K., Manimaran, D., Jayaraj, R. L., Elangovan, N., Dhivya, V., & Kaphle, A. (2015). Taxifolin curbs NF-κB-mediated Wnt/β-catenin signaling via up-regulating Nrf2 pathway in experimental colon carcinogenesis. Biochimie, 119, 103–112.
31. Oi, N., Chen, H., Kim, M. O., Lubet, R. A., Bode, A. M., & Dong, Z. (2012). Taxifolin suppresses UV-induced skin carcinogenesis by targeting EGFR and PI3K. Cancer Prevention Research, 5(9), 1103–1114.
32. Haque, M. W., Bose, P., Siddique, M. U. M., Sunita, P., Lapenna, A., & Pattanayak, S. P. (2018). Taxifolin binds with LXR (α & β) to attenuate DMBA-induced mammary carcinogenesis through mTOR/Maf-1/PTEN pathway. Biomedicine & Pharmacotherapy, 105, 27–36.
33. Haque, M. W., & Pattanayak, S. P. (2018). Taxifolin inhibits 7,12-dimethylbenz(a)anthracene-induced breast carcinogenesis by regulating AhR/CYP1A1 signaling pathway. Pharmacognosy Magazine, 13(Suppl), S749–S755.
34. Tutt, A. N., Garber, J. E., Kaufman, B., Viale, G., Fumagalli, D., Rastogi, P., ... & Geyer Jr, C. E. (2021). Adjuvant olaparib for patients with BRCA1-or BRCA2-mutated breast cancer. New England Journal of Medicine, 384(25), 2394-2405.